Semiconductor Physics, Quantum Electronics & Optoelectronics, 2025. V. 28, No 2. P. 215-220.

Optics

Ellipsometric study of $Ag_{6+x}(P_{1-x}Si_x)S_5I$ single crystals

A.I. Pogodin[1], M.M. Pop[1,2*], I.O. Shender[1], M.J. Filep[3], T.O. Malakhovska[1], O.P. Kokhan[1], K.V. Skubenych[1], V. Izai[4]

[1]*Uzhhorod National University, 46, Pidhirna str., 88000 Uzhhorod, Ukraine*
[2]*Institute for Information Recording, NAS of Ukraine, 88000 Uzhhorod Ukraine*
[3]*Ferenc Rákóczi II Transcarpathian Hungarian Institute, Kossuth Sq. 6, 90200 Beregovo, Ukraine*
[4]*Comenius University, Mlynska dolina, Bratislava 84248, Slovakia*
[*]*Corresponding author e-mail: mykhaylo.pop@uzhnu.edu.ua*

Abstract. Single crystals of $Ag_{6+x}(P_{1-x}Si_x)S_5I$ (x = 0, 0.25, 0.5, 0.75, 1) solid solutions were grown by directional crystallization from the melt. Grown crystals were investigated using XRD and spectral ellipsometry. $Ag_{6+x}(P_{1-x}Si_x)S_5I$ crystals are characterized by formation of a continuous series of solid solutions with a cubic F-43m structure. The studied samples had a nonlinear spectral dependence of the refractive index *n* and the extinction coefficient *k*. The presence of a sharp maximum of *n* and a rather sharp decrease in the *k* spectral dependences are observed within the 570…730 nm range. The spectral dependence of the refractive index was described by the single-oscillator Wemple–DiDomenico (WD) model. Parameters of the Wemple–DiDomenico model for $Ag_{6+x}(P_{1-x}Si_x)S_5I$ single crystals were determined. The effect of heterovalent cationic $P^{+5} \rightarrow Si^{+4}$ substitution on parameters of the Wemple–DiDomenico model was discussed.

Keywords: argyrodite, single crystal, refractive index, band gap.

https://doi.org/10.15407/spqeo28.02.215
PACS 78.20.Ci, 81.10.Fq

Manuscript received 14.03.25; revised version received 24.04.25; accepted for publication 11.06.25; published online 26.06.25.

1. Introduction

Ternary and quaternary silver-based argyrodites with the chemical formula $Ag_{12-x}E^{x+}Chal_{6-y}Hal_y$ (E^{x+} – Ga^{3+}, Si^{4+}, P^{5+}; Chal – S^{2-}, Se^{2-}, Te^{2-}; Hal – Cl^-, Br^-, I^-) have become notable materials in superionic and thermoelectric applications [1–5]. Recent studies have revealed that some ternary sulfides exhibit attractive photovoltaic and photocatalytic properties. It is reported that synthetic Ag_8SnS_6 in the form of nanocrystals or thin films has a band gap of E = 1.4 to 1.50 eV [6–8], while the band gap of the germanium-containing analogue Ag_8GeS_6 constitutes 1.4…1.466 eV [9, 10]. Meanwhile, quaternary argyrodites have higher values of band gap: from 1.527 eV (Ag_7GeS_5I) to 2.030 eV (Ag_6PS_5I) [11, 12]. Thus, potentially the first one meets a theoretical requirement of the Shockley–Queisser limit [13] for light absorbers in simple solar cells and the second for tandem cells [14].

Quaternary argyrodites crystalize in a cubic crystal system, SG F-43m with a similar cell parameter [15, 16]. A characteristic feature of argyrodite is the presence of a significant number of partially occupied cation positions (Ag^+), causing a disorder of the cationic sublattice. As a result, the appearance of the so-called Urbach tails is observed for argyrodites. The temperature and compositional dependence of Urbach tails in the solid solution based on quaternary argyrodites are reported in [11, 12]. The refractive index investigations of quaternary argyrodites are limited to $Ag_{6+x}(P_{1-x}Ge_x)S_5I$ and $Ag_7(Si_{1-x}Ge_x)S_5$. Also, these phases and their properties are the subject of theoretical calculations and molecular dynamics simulations [17–20] performed to better understand the influence of structure disordering on their properties.

This work aims to contribute to the optical characterization reported for single crystals of quaternary argyrodites by performing ellipsometry experiments for the first time.

2. Experimental

2.1. Sample preparation

The synthesis of $Ag_{6+x}(P_{1-x}Si_x)S_5I$ alloys (x = 0.25, 0.5, 0.75) was carried out from previously synthesized quaternary Ag_6PS_5I and Ag_7SiS_5I. Individual compounds were synthesized from high-purity elemental components of Ag (99.995%), P (99.9999%), or Si (99.9999%), S (99.999%), and previously synthesized AgI, taken in appropriate proportions in quartz ampoules evacuated to 0.13 Pa according to the procedure described in Refs. [16, 21]. The $Ag_{6+x}(P_{1-x}Si_x)S_5I$ alloys (x = 0.25, 0.5, 0.75) were synthesized by a direct one-temperature method in quartz ampoules evacuated to 0.13 Pa. The $Ag_{6+x}(P_{1-x}Si_x)S_5I$ samples were heated at the rate 50 °C/h to a maximum temperature of 950 °C. At this temperature, the samples were in the melt for 72 h. Subsequently, the samples were cooled to room temperature at a similar rate. As a

© V. Lashkaryov Institute of Semiconductor Physics of the NAS of Ukraine, 2025
© Publisher PH “Akademperiodyka” of the NAS of Ukraine, 2025

result, bulk polycrystalline alloys $Ag_{6.25}P_{0.75}Si_{0.25}S_5I$, $Ag_{6.5}P_{0.5}Si_{0.5}S_5I$, and $Ag_{6.75}P_{0.25}Si_{0.75}S_5I$ weighing 20 g each were obtained.

To establish the technological regimes (melt and annealing zone temperatures) of single crystal growth (Table 1), the obtained alloys were studied using differential thermal analysis (Pt/PtRh thermocouples, heating/cooling rate 700 °C/h). With account of the nature of the temperature behavior of $Ag_{6+x}(P_{1-x}Si_x)S_5I$ solid solutions, their single crystals were grown by the method of directional crystallization from melt-solution in a two-zone vertical resistance furnace. The single crystals were grown in evacuated quartz ampoules with a conical lower part. The single crystal growth regime included the following stages. (i) Formation of the nucleus in the lower conical part of the ampoule by the method of collective recrystallization for 48 h. (ii) The movement of the crystallization front at a rate of 0.5 mm/h. (iii) The annealing of the obtained single crystals for 72 h. (iv) The cooling of single crystals from the annealing temperature to room temperature at a rate of 5 °C/h. As a result, $Ag_{6+x}(P_{1-x}Si_x)S_5I$ single crystals of dark gray color with a metallic luster with a diameter of 1.2 cm and a length of 3 to 4 cm were obtained.

2.2. Methods

The $Ag_{6+x}(P_{1-x}Si_x)S_5I$ crystals were studied using X-ray diffraction (XRD) and spectral ellipsometry. For XRD analysis the AXRD Benchtop (Proto Manufacturing Limited) equipped with a DECTRIS MYTHEN2 R 1D detector, with Bragg–Brentano θ/2θ imaging geometry, Ni filtered CuKα radiation, 10…60° 2θ angle scanning range with a dynamic region of interest and 1 s exposure was used. The grown crystals were ground in an agate mortar and sieved to obtain a homogeneous powder. Powder patterns were indexed and lattice parameters were calculated in the EXPO 2014 program [22].

The spectral ellipsometry analysis of $Ag_{6+x}(P_{1-x}Si_x)S_5I$ single crystals was performed using the HORIBA Smart SE spectral ellipsometer, spectral range 440…1000 nm, beam angle 70°. The dispersion of the refractive index *n* and the extinction coefficient *k* were measured on plane-parallel single-crystal plates of $Ag_{6+x}(P_{1-x}Si_x)S_5I$ solid solutions polished to optical quality with a thickness of 0.2 mm at the temperature of 25 °C. The results were analyzed using the DeltaPsi2 software with the well-known Tauc–Lorenz model [23], which allows the determination of some important optical parameters using the Δ and Ψ parameters obtained as a result of measurements.

Table 1. Technological regimes for growing $Ag_{6+x}(P_{1-x}Si_x)S_5I$ single crystals.

Composition	Melt zone temperature, °C	Annealing zone temperature, °C
$Ag_{6.25}P_{0.75}Si_{0.25}S_5I$	870	550
$Ag_{6.5}P_{0.5}Si_{0.5}S_5I$	910	570
$Ag_{6.75}P_{0.25}Si_{0.75}S_5I$	925	580

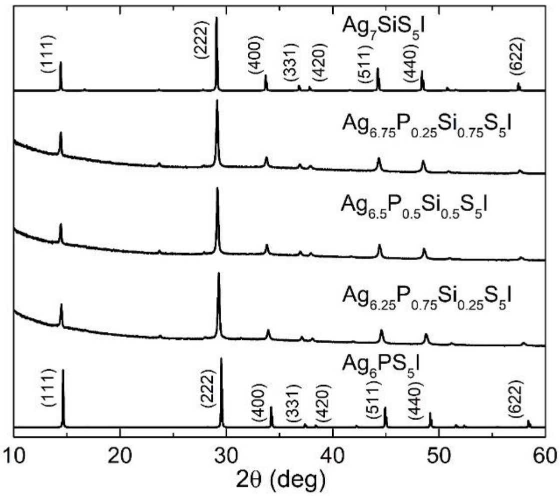

Fig. 1. Comparison of $Ag_{6+x}(P_{1-x}Si_x)S_5I$ solid solutions powder patterns.

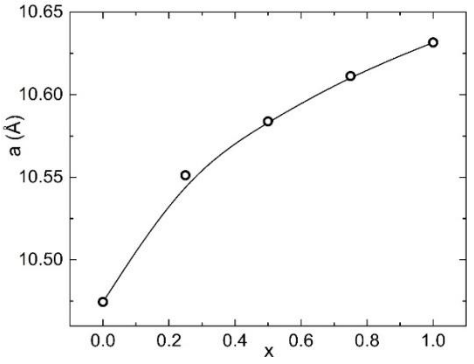

Fig. 2. Compositional dependence of lattice parameters for $Ag_{6+x}(P_{1-x}Si_x)S_5I$ solid solutions.

3. Results and discussion

As a result of comparison (Fig. 1) of the powder patterns of $Ag_{6+x}(P_{1-x}Si_x)S_5I$ (x = 0.25, 0.5, 0.75) with those of Ag_6PS_5I [16] and Ag_7SiS_5I [21], the presence of one system of diffraction peaks was established, indicating the formation of a continuous series of solid solutions and the absence of impurity phases.

Thus, the single crystals of $Ag_{6.25}P_{0.75}Si_{0.25}S_5I$, $Ag_{6.5}P_{0.5}Si_{0.5}S_5I$ and $Ag_{6.75}P_{0.25}Si_{0.75}S_5I$ solid solutions, as well as individual Ag_6PS_5I [16] and Ag_7SiS_5I [21] crystallize in the structure of argyrodite in the space SG F-43m, $Z = 4$.

It was found that the compositional behavior of the lattice parameters (Fig. 2) has a monotonic nonlinear character (positive deviation from Vegard's rule), indicating the disorder of the crystal structures of $Ag_{6+x}(P_{1-x}Si_x)S_5I$ solid solutions compared to Ag_6PS_5I and Ag_7SiS_5I.

It has been established that the spectral dependences of the refractive index for all the compositions of $Ag_{6+x}(P_{1-x}Si_x)S_5I$ solid solutions have a non-monotonic nonlinear character, which is expressed in the presence of a minimum and a maximum region (Fig. 3a). The presence of minimum regions (Fig. 3a) located within the wavelength range of ~ 470 to 560 nm (depending on the composition of the solid solutions) is associated with interband optical transitions, while the maximum regions (~ 570 to 730 nm) are located within the optical absorption edge [24, 25]. It should be noted that within the transparency range, with a further increasing the wavelength the refractive index decreases monotonically for all solid solution compositions (Fig. 3a). It is noteworthy that, in contrast to the refractive index *n*, the spectral behavior of the extinction coefficient *k* is more monotonous (Fig. 3b), manifesting in the decrease in the values of extinction coefficient *k* with increasing wavelength (within the transparency range).

Thus, the heterovalent cationic $P^{+5} \to Si^{+4}$ substitution in $Ag_{6+x}(P_{1-x}Si_x)S_5I$ single crystals leads to a monotonic insignificant (2.54…2.68) increase in the refractive index *n* (Fig. 4) determined within the transparency range (λ = 1000 nm).

Let us consider the spectral dependence of the refractive index *n* using the single-oscillator Wemple–DiDomenico (WD) model in detail, where the variance of refractive index is described by the following relation [26]:

$$n^2(E)-1=\frac{E_d^{\mathrm{WD}}E_0^{\mathrm{WD}}}{\left(E_0^{\mathrm{WD}}\right)^2-E^2}. \qquad (1)$$

where E_0^{WD} is the energy of a single-oscillator, E_d^{WD} is the dispersion energy.

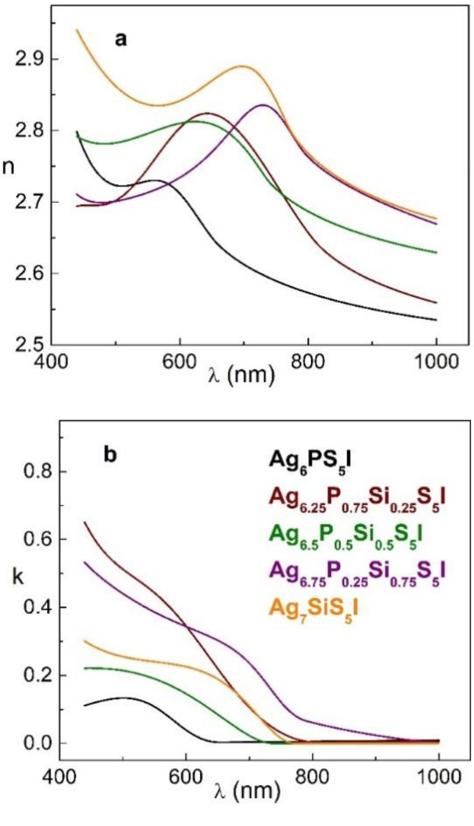

Fig. 3. Spectral dependences of refractive index *n* (a) and extinction coefficient *k* (b) for $Ag_{6+x}(P_{1-x}Si_x)S_5I$ crystals.

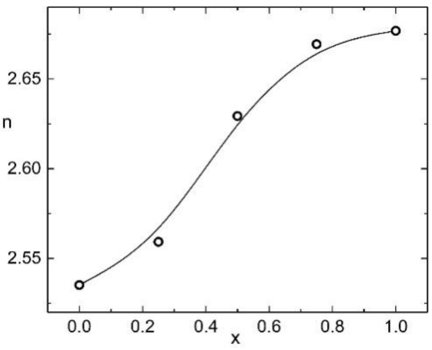

Fig. 4. Compositional dependence of the refractive index *n* for $Ag_{6+x}(P_{1-x}Si_x)S_5I$ single crystals.

The energy of a single-oscillator determines the spectral variation of the refractive index and describes the average energy of electrons transition between the highest energy levels of the valence band top and the lower levels of the conduction band in the band structure. Thus, using the WD model, the band gap E_g can be estimated as

$$E_0^{\mathrm{WD}} \approx 2E_g^{\mathrm{WD}}. \qquad (2)$$

It should be noted that the dispersion energy reflects the chemical nature and structure of the substance and characterizes the average strength of the interband optical transitions, which is shown by an empirical relation [27]:

$$E_d^{\mathrm{WD}} = \beta N_c Z_a N_e, \qquad (3)$$

where β is a constant, typically β = 0.37 ± 0.04 eV for compounds with a covalent bonds and β = 0.26 ± 0.04 eV for compounds with an ionic bonds, N_c is the coordination number of the cation in the anionic polyhedron, N_e is the total number of valence electrons per anion, Z_a is the anion oxidation state.

Considering the above equations, one can summarize that the dispersion energy is associated with changes in the structural order of the material (the degree of ionic bonding, anion's oxidation state, the coordination number in the structural polyhedra, *etc.*) [28, 29].

The values of the static (constant at an infinite wavelength) refractive index n_0^{WD} and ionicity f_i^{WD} were calculated within the Wemple–DiDomenico model by using equations (4) and (5), respectively [29]:

Table 2. Parameters of the Wemple–DiDomenico model for $Ag_{6+x}(P_{1-x}Si_x)S_5I$ single crystals.

Composition	E_0^{WD} (eV)	E_d^{WD} (eV)	E_g^{WD} (eV)	n_0^{WD}	f_i^{WD}
Ag_6PS_5I	5.17	26.49	2.59	2.47	0.44
$Ag_{6.25}P_{0.75}Si_{0.25}S_5I$	4.85	25.46	2.43	2.50	0.44
$Ag_{6.5}P_{0.5}Si_{0.5}S_5I$	4.38	23.80	2.19	2.53	0.43
$Ag_{6.75}P_{0.25}Si_{0.75}S_5I$	3.88	21.39	1.94	2.55	0.42
Ag_7SiS_5I	3.72	20.60	1.86	2.56	0.42

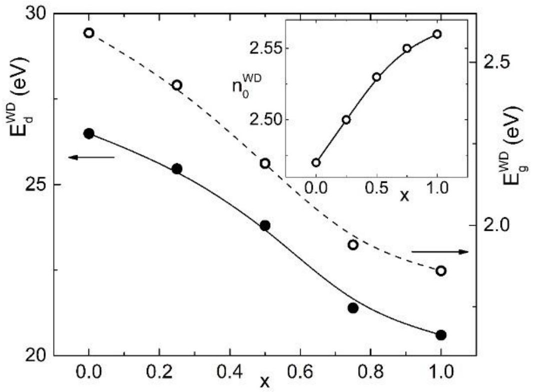

Fig. 5. Compositional dependences of the dispersion energy E_d^{WD} and the estimated band gap values E_g^{WD} for $Ag_{6+x}(P_{1-x}Si_x)S_5I$ single crystals. The inset shows the compositional dependence of the static refractive index n_0^{WD}.

$$n_0^{WD} = \left[1 + \frac{E_d^{WD}}{E_0^{WD}}\right]^{1/2}, \tag{4}$$

$$f_i^{WD} = \left[\frac{E_0^{WD}}{E_d^{WD}}\right]^{1/2}. \tag{5}$$

All the parameters calculated within the Wemple–DiDomenico model for $Ag_{6+x}(P_{1-x}Si_x)S_5I$ single crystals are shown in Table 2.

Thus, it was found that the heterovalent cationic $P^{+5} \to Si^{+4}$ substitution leads to a monotonic nonlinear decrease in the values of E_0^{WD} (Table 2), E_d^{WD}, and E_g^{WD} (Fig. 5), and an increase in the values of the static refractive index n_0^{WD} (inset of Fig. 5), while the values of ionicity f_i^{WD} practically do not change (Table 2).

The decrease in the energy of a single-oscillator E_0^{WD} (Table 2) and, as a consequence, the band gap values E_g^{WD} (Fig. 5) are associated with the changes in $Ag_{6+x}(P_{1-x}Si_x)S_5I$ band structure. Since, the optical parameters of $Ag_{6+x}(P_{1-x}Si_x)S_5I$ are mainly responsible for the tetrahedra $[PS_4]$ (Ag_6PS_5I), $[SiS_4]$ (Ag_7SiS_5I) and $[P(Si)S_4]$ $(Ag_{6+x}(P_{1-x}Si_x)S_5I$ (x = 0.25; 0.5; 0.75)), which emerging from (Eq. (3)) and the results of calculating ionicity f_i^{WD} (Table 2), one can summarize the following. The decrease in the values of dispersion energy E_d^{WD} (Fig. 5) induced by the heterovalent cationic $P^{+5} \to Si^{+4}$ substitution is associated with a gradual decrease in the number of valence electrons N_e from 11 ($[PS_4]$ tetrahedron) to 10 ($[SiS_4]$ tetrahedron) since the other parameters (Eq. (3)) for the above tetrahedra will not change.

4. Conclusions

Grown using the directional crystallization $Ag_{6+x}(P_{1-x}Si_x)S_5I$ (x = 0, 0.25, 0.50, 0.75, 1) crystals were studied using the powder XRD and spectral ellipsometry methods. It has been ascertained that all studied samples crystallize in a cubic SG F-43m, indicating the formation of a continuous series of solid solutions. The lattice parameters of $Ag_{6+x}(P_{1-x}Si_x)S_5I$ were determined. The spectral dependences of the refractive index n and the extinction coefficient k were investigated. The obtained results were analyzed within the Tauc–Lorenz model. To describe the dependences of the refractive index and calculate the single-oscillatory E_0^{WD} and dispersion E_d^{WD} energies, the Wemple–DiDomenico single-oscillatory model was used. It was ascertained that the heterovalent cationic $P^{+5} \to Si^{+4}$ substitution induces the monotonic nonlinear decrease in the compositional dependences of E_0^{WD} and E_d^{WD}.

Acknowledgements

The authors also thank the Armed Forces of Ukraine for providing security to perform this work. This work has become possible only because of the resilience and courage of the Ukrainian Army.

References

1. Lin S., Li W., Pei Y. Thermally insulative thermoelectric argyrodites. *Mater. Today*. 2021. **48**. P. 198–213. https://doi.org/10.1016/j.mattod.2021.01.007.
2. Laqibi M., Cros B., Peytavin S., Ribes M. New silver superionic conductors Ag_7XY_5Z (X = Si, Ge, Sn; Y = S, Se; Z = Cl, Br, I)-synthesis and electrical studies. *Solid State Ionics*. 1987. **23**. P. 21–26. https://doi.org/10.1016/0167-2738(87)90077-4.
3. Studenyak I.P., Pogodin A.I., Shender I.A. *et al.* Electrical properties of ceramics based on Ag_7TS_5I (T = Si, Ge) solid electrolytes. *J. Solid State Chem.* 2022. **309**. P. 122961. https://doi.org/10.1016/j.jssc.2022.122961.
4. Pogodin A.I., Filep M.J., Izai V.Yu. *et al.* Crystal growth and electrical conductivity of Ag_7PS_6 and Ag_8GeS_6 argyrodites. *J. Phys. Chem. Solids*. 2022. **168**. P. 110828. https://doi.org/10.1016/j.jpcs.2022.110828.
5. Wang B., Li S., Luo Y. *et al.* A new thermoelectric Ag_8SiSe_6 argyrodite for room temperature application: sensitivity of thermoelectric performance to cooling conditions. *Mater. Adv.* 2024. **5**. P. 3735–3741. https://doi.org/10.1039/d3ma01190a.
6. Boon-on P., Aragaw B.A., Lee C.-Y. *et al.* Ag_8SnS_6: A new IR solar absorber material with a near optimal bandgap. *RSC Adv.* 2018. **8**. P. 39470–39476. https://doi.org/10.1039/C8RA08734B.
7. Hu W.-Q., Shi Y.-F., Wu L.-M. Synthesis and shape control of Ag_8SnS_6 submicropyramids with high surface energy. *Cryst. Growth Des.* 2012. **12**, No 7. P. 3458–3464. https://doi.org/10.1021/cg201649d.
8. Zhu L., Xu Y., Zheng H. *et al.* Application of facile solution-processed ternary sulfide Ag_8SnS_6 as light absorber in thin film solar cells. *Sci. China Mater.* 2018. **61**. P. 1549–1556. https://doi.org/10.1007/s40843-018-9272-3.
9. Li Z., Liu C., Zhang X. *et al.* An easily prepared Ag_8GeS_6 nanocrystal and its role on the performance enhancement of polymer solar cells. *Org. Electron.* 2017. **45**. P. 247–255. https://doi.org/10.1016/j.orgel.2017.03.029.
10. Pogodin A., Pop M., Shender I. *et al.* Anionic framework descriptors and microstructure affects on

optical parameters of $Ag_{7+x}(P_{1-x}Ge_x)S_6$ single crystals. *Opt. Mater.* 2023. **145**. P. 114407. https://doi.org/10.1016/j.optmat.2023.114407.

11. Pogodin A.I., Pop M.M., Shender I.O. *et al.* Effect of structural site disorder on the optical properties of $Ag_{6+x}(P_{1-x}Ge_x)S_5I$ solid solutions. *J. Mater. Sci.: Mater. Electron*. 2022. **33**. P. 21874–21889. https://doi.org/10.1007/s10854-022-08974-4.
12. Pogodin A.I., Pop M.M., Shender I.A. *et al*. Influence of order–disorder effects on the optical parameters of $Ag_7(Si_{1-x}Ge_x)S_5I$-mixed crystals. *J. Mater. Sci.: Mater. Electron*. 2022. **33**. P. 15054–15066. https://doi.org/10.1007/s10854-022-08422-3.
13. Sutherland B.R. Solar materials find their band gap. *Joule*. 2020. **4**. P. 984–985. https://doi.org/10.1016/j.joule.2020.05.001.
14. Peters I.M., Rodríguez Gallegos C.D., Lüer L., Hauch J.A. *et al.* Practical limits of multijunction solar cells. *Prog. Photovolt. Res. Appl*. 2023. **31**, No 10. P. 1006–1015. https://doi.org/10.1002/pip.3705.
15. Kuhs W.F., Nitsche R., Scheunemann K. The argyrodites – a new family of tetrahedrally close-packed structures. *Mat. Res. Bull.* 1979. **14**. P. 241–248. https://doi.org/10.1016/0025-5408(79)90125-9.
16. Studenyak I.P., Pogodin A.I., Filep M.J. *et al*. Crystal structure and electrical properties of Ag_6PS_5I single crystal. *SPQEO*. 2021. **24**. P. 26–33. https://doi.org/10.15407/spqeo24.01.026.
17. Kashuba A.I., Andriyevsky B., Semkiv I.V. *et al*. Impact of structure on the vibrational properties of Ag_8SnSe_6 crystal: Experimental and theoretical studies. *Opt. Mater.: X*. 2022. **15**. P. 100180. https://doi.org/10.1016/j.omx.2022.100180.
18. Munsif M., Neffati R., Shah M. *et al*. First principles study of the structural, mechanical and optical properties of argyrodite-structured Ag_6PS_5X (X = Br, I) compounds. *Solid State Commun*. 2023. **371**. P. 115245. https://doi.org/10.1016/j.ssc.2023.115245.
19. Semkiv I., Ilchuk H., Kashuba N. *et al*. Synthesis, crystal and energy structure of the Ag_8SnS_6 crystal. *Phys. Chem. Solid State*. 2023. **24**, No 3. P. 441–447. https://doi.org/10.15330/pcss.24.3.441-447.
20. Wei P.-C., Hsing C.-R., Yang C.-C. *et al*. Liquid-like thermal conductivity in solid materials: Dynamic behavior of silver ions in argyrodites. *Nano Energy*. 2024. **122**. P. 109324. https://doi.org/10.1016/j.nanoen.2024.109324.
21. Pogodin A.I., Studenyak I.P., Shender I.A. *et al*. Crystal structure, ion transport and optical properties of new high-conductivity $Ag_7(Si_{1-x}Ge_x)S_5I$ solid solutions. *J. Mater. Sci.* 2022. **57**. P. 6706–6722. https://doi.org/10.1007/s10853-022-07059-1.
22. Altomare A., Cuocci C., Giacovazzo C., Moliterni A. *et al*. EXPO2013: a kit of tools for phasing crystal structures from powder data. *J. Appl. Crystallogr*. 2013. **46**. P. 1231–1235. https://doi.org/10.1107/S0021889813013113.
23. Jellison G.E., Modine F.A. Parameterization of the optical functions of amorphous materials in the interband region. *Appl. Phys. Lett.* 1996. **69**, No 3. P. 371–373. https://doi.org/10.1063/1.118064.
24. Howlader C., Hasan M., Zakhidov A., Chen M.Y. Determining the refractive index and the dielectric constant of PPDT2FBT thin film using spectroscopic ellipsometry. *Opt. Mater.* 2020. **110**. P. 110445. https://doi.org/10.1016/j.optmat.2020.110445.
25. Muhammad F.F., Yahya M.Y., Aziz F. *et al*. Tuning the extinction coefficient, refractive index, dielectric constant and optical conductivity of Gaq3 films for the application of OLED displays technology. *J. Mater. Sci. Mater. Electron*. 2017. **28.** P. 14777–14786. https://doi.org/10.1007/s10854-017-7347-y.
26. Wemple S.H., DiDomenico M. Behavior of the electronic dielectric constant in covalent and ionic materials. *Phys. Rev. B.* 1971. **3**. P. 1338–1352. https://doi.org/10.1103/physrevb.3.1338.
27. Wemple S.H. Refractive-index behavior of amorphous semiconductors and glasses. *Phys. Rev. B.* 1973. **7**. P. 3767. https://doi.org/10.1103/PhysRevB.7.3767.
28. Tanaka K. Optical properties and photoinduced changes in amorphous As-S films. *Thin Solid Films.* 1980. **66**. P 271–279. https://doi.org/10.1016/0040-6090(80)90381-8.
29. Tubbs M.S. A spectroscopic interpretation of crystalline ionicity. *phys. status solidi* (*b*). 1970. **41**. P. k61–k64. https://doi.org/10.1002/pssb.19700410164.

Authors and CV

Artem I. Pogodin, PhD, Associate Professor and Senior Researcher at the Uzhhorod National University. Authored over 100 scientific papers and 114 patents. The area of his scientific interests includes solid state chemistry, crystal growth and materials science.
E-mail: artempogodin88@gmail.com,
https://orcid.org/0000-0002-2430-3220

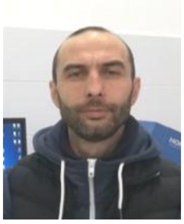

Mykhailo M. Pop, PhD, Lecturer and Researcher at the Uzhhorod National University. Authored nearly 100 publications. The area of his scientific interests includes physical and optical properties of semiconductors, superionic materials, chalcogenide glasses and films.
https://orcid.org/0000-0003-3674-3482

Iryna O. Shender, defended her PhD thesis at the Uzhhorod National University in 2024. Authored 33 scientific papers and 7 patents. The area of her scientific interests is electrical, optical and mechanical properties of superionic conductors.
E-mail: shender95@gmail.com,
https://orcid.org/0000-0003-1687-3634

Mykhailo J. Filep, PhD, Associate Professor at the Ferenc Rákóczi II Transcarpathian Hungarian Institute. Authored over 100 scientific papers and 50 patents. The area of his scientific interests includes solid state chemistry and materials science.
E-mail: mfilep23@gmail.com,
http://orcid.org/0000-0001-7017-5437

Tetyana O. Malakhovska, PhD, Senior Researcher at the Uzhhorod National University. Authored 70 scientific papers and 10 patents. The area of her scientific interests includes solid state chemistry and materials science.
E-mail: t.malakhovska@gmail.com,
https://orcid.org/0000-0001-7309-4894

Oleksandr P. Kokhan, PhD, Associate Professor at the Uzhhorod National University. Authored over 80 scientific papers and 95 patents. The area of his scientific interests includes inorganic chemistry, solid state chemistry, crystal growth, and materials science. E-mail: aleksandr.kokh@gmail.com,
http://orcid.org/0000-0003-1534-6779

Kateryna V. Skubenych, PhD, Head of the Research and Development department of the State Higher Education Establishment “Uzhhorod National University”. Author of 9 articles and 3 patents. Research interests: research of mechanical properties of super-ionic crystals, solid solutions, compo-sites and ceramics by micro- and nanoindentation methods.
E-mail: katjaskubenytch@gmail.com,
https://orcid.org/0000-0001-9518-2086

Vitalii Yu. Izai, PhD in Physics of Semiconductors and Dielectrics. Scientific Associate at the Faculty of Mathematics, Physics and Informatics, Comenius University Bratislava. Authored 40 articles and more than 20 patents. The area of his interests includes materials science, superionic materials for solid-state ionics, deposition and physical properties of thin films.
E-mail: vitalii.izai@fmph.uniba.sk,
https://orcid.org/0000-0001-7512-3388

Authors’ contributions

Pogodin A.I.: supervision, conceptualization, investiga-tion, writing – original draft.
Pop M.M.: investigation, writing – original draft.
Shender I.O.: investigation, visualization.
Kokhan O.P.: visualization, conceptualization.
Filep M.J.: methodology, visualization, writing – review & editing.
Malakhovska T.O.: investigation, writing – original draft.
Skubenych K.V.: methodology, investigation.
Izai V.: methodology, writing – review & editing.

Еліпсометричне дослідження монокристалів $Ag_{6+x}(P_{1-x}Si_x)S_5I$

А.І. Погодін, М.М. Поп, І.О. Шендер, М.Й. Філеп, Т.О. Малаховська, О.П. Кохан, К.В. Скубенич, В. Ізай

Анотація. Монокристали твердих розчинів $Ag_{6+x}(P_{1-x}Si_x)S_5I$ (x = 0, 0.25, 0.5, 0.75, 1) вирощували методом спрямованої кристалізації з розплаву. Вирощені кристали досліджували методами рентгенівського фазового аналізу та спектральної еліпсометрії. Кристали $Ag_{6+x}(P_{1-x}Si_x)S_5I$ характеризуються утворенням неперервного ряду твердих розчинів з кубічною структурою F-43m. Досліджувані зразки мають нелінійну спектральну залежність показника заломлення *n* і коефіцієнта екстинкції *k*. В області 570…730 нм спостерігається наявність різкого максимуму для *n* і досить різкий спад спектральних залежностей *k*. Спектральна залежність показника заломлення описується одно-осциляторною моделлю Вемпла–ДіДоменіко. Визначено параметри моделі Вемпла–ДіДоменіко для монокристалів $Ag_{6+x}(P_{1-x}Si_x)S_5I$. Обговорено вплив гетеровалентного катіонного заміщення $P^{+5} \rightarrow Si^{+4}$ на параметри моделі Вемпла–ДіДоменіко.

Ключові слова: аргіродит, монокристал, показник заломлення, заборонена зона.